

Comparative Histological and Immunohistochemical Study on the Effect of Platelet-Rich Plasma, Adipose Tissue Derived Mesenchymal Stem Cells, and Mesenchymal Stem Cells Derived Exosomes in Experimentally Induced Corneal Alkali Burn in Albino Rats

Sahar Ezzat Nasr, Amal Elham Fares, Eman Ahmed Al-Sayed and Asmaa Ahmed El-Shafei

Department of Medical Histology & Cell Biology, Faculty of Medicine, Cairo University, Egypt

ABSTRACT

Background and Objectives: Alkali damage to the cornea can be catastrophic and results in lifelong pain and visual loss. Investigation and comparison of the potential therapeutic effects of platelet-rich plasma (PRP), adipose tissue derived mesenchymal stem cells (ADSCs), and mesenchymal stem cells derived exosomes (MSCs-EX) in experimentally induced corneal alkali burn in rats were the goal of this work.

Material and Methods: 60 adult male albino rats were divided into: Donor group; 10 rats, Group I (Control group); 10 rats, and Group II (Alkali burn group); 40 rats. All rats of group II received right eyes corneal alkali burn by sodium Hydroxide (NaOH), then equally subdivided into: Subgroup II-a (spontaneous recovery subgroup): left untreated, Subgroup II-b (PRP treated subgroup): received a single subconjunctival injection of 0.5 ml PRP 2 hours after alkali burn, Subgroup II-c (ADSCs treated subgroup): received a single subconjunctival injection of 1.3×10^5 AMSCs; 1 hour after alkali burn and Subgroup II-d (MSCs-EX treated subgroup): received a single subconjunctival injection of 100 μ g protein/mL MSCs-EX; 1 hour after alkali burn. Rats were sacrificed after 3 weeks, then right eyes' corneas were excised for histological, morphometric, and statistical analysis.

Results: Deterioration of corneal histological architecture was detected in subgroup II-a, in the form of degeneration and desquamation of corneal epithelial and endothelial cells, degenerated keratocytes and disrupted corneal stroma with expressed neovascularization and cellular infiltration. Treatment with either PRP, ADSCs and MSCs-EX showed different degrees of improvement, in the form of regeneration of corneal epithelium, endothelium and corneal stroma with disappearance of neovascularization and cellular infiltration.

Conclusion: PRP, ADSCs and MSCs-EX treatment significantly ameliorated corneal degenerative changes induced by alkali burn by their anti-inflammatory, anti-angiogenic and anti-apoptotic properties; with a more pronounced improvement in response to MSCs-EX.

Received: 20 February 2023, **Accepted:** 15 March 2023

Key Words: ADSCs, corneal alkali burn, MSCs-EX, PRP, VEGF.

Corresponding Author: Asmaa Ahmed El-Shafei, MD, Department of Medical Histology & Cell Biology, Faculty of Medicine, Cairo University, Egypt, **Tel.:** +20 10 9014 7994, **E-mail:** asmaashafei@kasralainy.edu.eg

ISSN: 1110-0559, Vol. 47, No. 1

INTRODUCTION

One of the most challenging eye injuries is the acute ocular chemical burn, which accounts for 11.5 to 22.1 % of ocular injuries and constitutes ophthalmic emergency^[1]. Nearly 60% of all chemical eye injuries are caused by burns from alkalis. The cornea and conjunctiva might be damaged right away when the alkali comes into touch with the ocular surface. The corneal stroma's highly organized collagen bundles and proteoglycan ground material are both destroyed by alkali, and the constant synthesis of proteases from the injured tissue results in significant tissue damage^[2]. In addition to corneal ulceration, neovascularization and opacification with sluggish epithelial regeneration could also occur. Finally, it might result in irreversible vision loss or possible corneal blindness^[3].

Steroids, nonsteroidal anti-inflammatory agents, citrate, artificial tears, photodynamic therapy, argon laser photocoagulation, collagenase inhibitors, conjunctival transplantation, topical fibronectin, therapeutic contact lenses, amniotic membrane repairing, and limbal transplantation are all among the medical and surgical treatment options for corneal alkali burn. These methods are occasionally ineffectual, particularly for significant corneal neovascularization (CNV) induced by inflammation, and hence attention is turned toward alternate therapy approaches to eliminate such potentially harmful downsides^[4].

Platelet-rich plasma (PRP) is a popular treatment in ophthalmology, plastic and reconstructive surgery, skin burns, and trauma^[5]. PRP is a non-toxic and non-

immunogenic blood component derived by centrifuging blood as whole to obtain a cellular constituent of platelet rich plasma, which contains hepatocyte growth factor, insulin-like growth factors (1 and 2), fibroblast growth factor, transforming growth factor, and vascular endothelial growth factor. Furthermore, it contains bioactive substances or non-growth factors such as histamine, serotonin, adenosine, calcium, dopamine, fibrin, vitronectin, and fibronectin. All these factors are proposed to induce soft tissue healing by accelerating regeneration of epithelial and endothelial cells, inducing angiogenesis, improving hemostasis, increasing collagen synthesis, and assisting cell migration and differentiation^[6].

One type of mesenchymal stem cell that is prevalent in humans are adipose-derived mesenchymal stem cells (ADSCs). They are multipotent adult stem cells derived from adipose tissue with the ability to self-regenerate and differentiate into numerous cell lineages^[7,8]. Because adipose tissue is easy to obtain and handle, ADSCs have been used for regeneration, tissue engineering processes and wound repair; also in *vitro*, the separated cells rapidly multiply and develop into diverse cell types^[9].

Exocytosis produces exosomes (EX). They are tiny vesicles for transmitting genetic information that have a bilipid membrane, a diameter of 30 to 150 nm, and a lot of proteins, lipids, mRNAs (messenger Ribonucleic acid), and microRNAs^[10]. They play a crucial role in communication between cells through protein and RNA transport, are secreted by all cell types, and are found in urine, blood, and breast milk^[11,12]. Under normal circumstances, they are released biologically, but pathological circumstances like degeneration and malignancies speed up their rate of release^[13]. Exosomes are being used to treat a variety of disorders, including acute renal injury, liver fibrosis, wound healing, myocardial infarction, and ischemia-induced brain degeneration^[14]. The aim of this work was to investigate and compare the possible effect of PRP, ADSCs and MSCs-EX in experimental corneal alkali burn in albino rats.

MATERIALS AND METHODS

Drugs

Sodium Hydroxide (NaOH): as a white powder from the El-Gomhoria Chemicals Company in Cairo, Egypt. Corneal alkali burn was induced by dissolving one mole (= 4 g) of pure NaOH in one liter of water^[15].

Animals

This study is conducted on 60 male adult albino rats about, which were about 12 weeks old, their body weight ranged from 150 – 250 grams. Rats were housed in stainless-steel cages (5 rats in each cage) in Kasr Al-Ainy's animal house of Faculty of Medicine, Cairo University. They were handled in accordance with standards that the Cairo University Animal Use Committee had approved with the approval number (CU III F 39 20), under typical ambient conditions, with unrestricted access to a standard diet and water over the study time.

Experimental design

The rats were randomly divided into

Donor group (n:10): Rats were used for obtaining blood needed in PRP preparation & for both ADSCs & MSCs-EX isolation, culture, phenotyping, and labeling.

Group I (Control group) (n:10): One subconjunctival injection of PBS (equivalent to 0.2 ml) was administered to rats' right eyes.

Group II (Alkali burn group) (n:40): Each rat's right eye received a corneal alkali burn by NaOH (as will be mentioned later). After establishment of corneal ulceration by the slit lamp microscope in the Ophthalmology department, Faculty of medicine, Cairo university, rats were equally subdivided into:

Subgroup II-a (spontaneous recovery subgroup) (n:10): Rats were left untreated.

Subgroup II-b (PRP treated subgroup) (n:10): Two hours after the alkali burn, each rat's right eye received a single subconjunctival dose of 0.5 ml of PRP^[16].

Subgroup II-c (ADSCs treated subgroup) (n:10): One hour after the alkali burn, each rat's right eye received a single subconjunctival injection of 1.3×10^5 cultured and green fluorescent protein (GFP)-labeled ADSCs suspended in 0.2 ml PBS^[4].

Subgroup II-d (MSCs-EX treated subgroup) (n:10): One hour after the alkali burn, each rat's right eye was injected sub-conjunctively with a single dose of 100 µg protein/mL GFP-labelled MSCs-EX diluted with 0.2 ml PBS^[17].

In subgroups II-c & II-d, three days following injection, 5 rats were sacrificed to ensure homing of both ADSCs & MSCs-EX respectively^[18]. While the remaining rats of both groups I & II were sacrificed 3 weeks after the beginning of the experiment.

Induction of Corneal alkali burn by NaOH

Half mg/kg of ketamine was administered intramuscularly to anaesthetize the rats. After that, round filter papers rinsed by NaOH (1N) were used to cover the rats' corneal surfaces of right eyes for 45 seconds. After that, 0.9 percent physiological saline was used to clean the wound's surface. The entire cornea was covered in filter paper (7 mm in diameter). Immediately after the corneal alkali injury, rats were submitted to ophthalmologic examination by bio-microscopy in a slit lamp to confirm corneal ulceration. To enable the rats to move and eat without restriction, the other eye was left unburned^[15]. All rats subjected to corneal ulcer received levofloxacin eye drops and topical antibiotic twice daily over the experiment duration^[19].

Steps of PRP preparation^[20]

In the Biochemistry Department of faculty of medicine, Cairo University, PRP extract was freshly prepared. Ten

age-matched healthy male albino rats were used to prepare the PRP. Four ml of blood was obtained from each rat tail vein, which was then transferred into test tubes containing 3.2 percent sodium citrate (Merck, Darmstadt, Germany) at a 9/1 blood to citrate ratio. A centrifuge (5810 R, Eppendorf AG, Hamburg, Germany) was used to centrifuge the blood for 10 minutes at 400 g, after which the supernatant was transferred to another tube & centrifuged once again for 10 minutes at 800g. Platelet-poor plasma (PPP) made up the top two-thirds, which were eliminated. The final layer, or 1/3 of it, was regarded as PRP. PRP was allotted and stored at -20 °C for future use.

Isolation, propagation, and characterization of ADSCs^[21]

ADSCs were prepared in the Biochemistry Department of faculty of medicine, Cairo University. Subcutaneous white adipose tissue was taken out of a rat's inguinal fat pad under extremely sterile circumstances. After being removed, the adipose tissue was kept into a sterile tube with 15 ml phosphate buffered solution (PBS; Gibco/Invitrogen, Grand Island, New York, USA). Hank's Balanced Salt Solution was subjected to an enzyme digestion procedure employing 0.075 percent collagenase II (Serva Electrophoresis GmbH, Mannheim) for one hour at 37°C with moderate shaking. Erythrocytes were eliminated from digested tissue by treating it with erythrocyte lysis buffer after it had been filtered and centrifuged. Dulbecco Modified Eagle Medium (DMEM; Gibco/BRL, Grand Island, New York, USA, Cat. No. 10565018) supplemented with 10% fetal bovine serum was used to transfer cells to tissue culture flasks. Non-adherent cells were then eliminated using a PBS wash following a 24-hour attachment period. Attached cells were grown in *vitro* after being cultivated in DMEM media supplemented with 10% fetal bovine serum (FBS), 1.25 mg/L amphotericin B, and 1% penicillin-streptomycin (Gibco/BRL, Cat. No. 15240062). Cultures were trypsinized with 0.25 percent trypsin in 1 mM EDTA (Gibco/BRL, Cat. No. 25200056) for 5 minutes at 37°C. after being rinsed twice with PBS at 80–90% confluence. Cells were centrifuged, resuspended in media containing serum, and then incubated in a culture flask (50 cm²) (Falcon, Product No. C000025). First-passage cultures were created as a result, and they were in *vitro* expanded until passage four. By Flow cytometry, CD29, one of the rat ADSC surface markers (ab93758, Abcam, Cambridge, United Kingdom), was used to characterize ADSCs.

Isolation and characterization of MSCs-EX^[22]

Fourth generation ADSCs were cultivated for 48 h in DMEM/F12 supplemented with 10% exosome depleted FBS, and the supernatants were collected carefully. For exosome isolation, first centrifugations were done at 4°C for the following durations: 500 g for 10 min, 2000 g for 10 min, and 12,000 g for 30 min. Each time, the supernatant was kept. After the pellet was resuspended in PBS to remove any leftover soluble components, the supernatant was centrifuged at 120,000 g for 70 min at 4°C. This was

followed by another ultra-centrifugation at 120,000 g for 70 min at 4°C. The last pellet was reconstituted in 200 cc of PBS and stored at -80°C until their appropriate injection time. Transmission electron microscopy (TEM) was used to examine the morphology of the isolated exosomes, and nanoparticle tracking analysis was used to evaluate the distribution of size (NTA; Zeta View system). Further characterization of exosomal markers CD81, CD63, and CD9 (ab275018, Abcam, Cambridge, United Kingdom) was done by Flow cytometry.

Labeling of ADSCs & MSCs-EX with GFP^[23]

During the 4th passage, ADSCs and the isolated exosomes were harvested and labeled with GFP to detect their homing in the corneal tissue using a fluorescent microscope on unstained corneal sections.

Histological study

Rats were sacrificed under lethal dose of general anesthesia by phenobarbitone (80 mg /kg) intraperitoneal injection^[24]. The corneas of the right eyes from each group were fixed in 10% formol saline & embedded in paraffin. Sections of 7 m thick were cut and stained by the following stains:

- a. Hematoxylin and Eosin (H & E) stain^[25] to examine the histological structure of the cornea in different groups.
- b. Masson's trichrome stain^[26] for demonstration of collagen fibers.
- c. Periodic acid schiff reaction (PAS)^[26] to examine Bowman's membrane and Descemet's membrane changes.
- d. Immunohistochemical staining with avidin–biotin peroxidase complex technique^[27] for:
 1. Vascular endothelial growth factor (VEGF); a neovascularization marker. It is a ready to use mouse monoclonal human reactive VEGF Ab (Product Code: NCL-L-VEGFR-3, Leica Bio systems, Newcastle Ltd Balliol Business Park Benton Lane UK). VEGF positive cells showed membranous/cytoplasmic brown reaction.
 2. Anti P53 antibody; a marker for cell apoptosis to detect p53 protein that regulates cell cycle and death^[28]. It is a ready to use rabbit polyclonal antibody (ab16665, Abcam plc, Cambridge, UK). P53 positive cells showed brown membranous/cytoplasmic deposits.

Application of the primary antibodies was followed by incubation in a humid chamber at room temperature for 60 min. A human placenta, breast and colon were used as +ve control specimens for VEGF, PCNA and P53 respectively according to the data provided by the antibodies manufacturer. One of the corneal sections was used as –ve control by omitting the step of the primary antibody.

Morphometric Study

Data were collected and analyzed using a computer system called "Leica Qwin 500C" for image analysis (Leica Imaging System Ltd, Cambridge, UK) at Medical Histology and Cell Biology department, Faculty of medicine, Cairo university. The following parameters were measured in ten non-overlapping randomly chosen fields (x100 magnification measuring frame 116964.91 μm^2) for each animal:

- Mean central corneal thickness in H & E-stained sections.
- Mean area % of collagen in Masson's trichrome stained sections.
- Mean gray of PAS reaction (Optical density of PAS staining).
- Mean number of immunopositive cells for VEGF and P53.

Statistical Analysis^[29]

Data were collated and statistically evaluated to determine differences between the research groups in terms of the various parameters. Correlations between the important researched parameters were examined. The arithmetic mean, standard deviation, and analysis of variance were all part of the statistical study (ANOVA). The computer instantly supplied the probability (p) value determined from statistical tables using the Statistical Package for Social Sciences (SPSS) software version 21. When (p) was less than 0.05, the results were regarded as statistically significant.

RESULTS

No mortality was reported all through the experiment period.

Immunofluorescent Results

ADSCs and MSCs-EX displayed intense green fluorescence, demonstrating that they had been seeded into corneal tissue. In the corneal stroma, several immunostained ADSCs and MSCs-EX were found, and some cells were found in the limbus (Figures 1a,b respectively).

Histological results

Hematoxylin and Eosin-Stained Sections

Corneal sections of the control group (Group I) showed normal histological landmarks of the five different layers of cornea; non-keratinized stratified squamous epithelium, Bowman's membrane, substantia propria with regularly arranged collagen bundles and flattened pale nuclei of keratocytes scattered in-between, homogenous non cellular Descemet's membrane and finally a single layer of flattened endothelial cells with flattened nuclei (Figure 2a).

Corneal sections from untreated alkali burn (spontaneous recovery) subgroup (Subgroup II-a) showed corneal epithelial changes ranging from desquamation in

some parts to marked separation in others with flat basal cells. Desquamation and degeneration of superficial cells, in addition to multiple epithelial cells with vacuolated cytoplasm and dark nuclei were observed. Some parts of the substantia propria exhibited separated and disturbed collagen bundles with multiple degenerated keratocytes, neovascularization & inflammatory cellular infiltration in-between. Disruption and separation of Descemet's membrane with endothelial cells lost in some fields were also seen (Figure 2b).

Sections from PRP treated subgroup (Subgroup II-b) revealed a disturbed corneal structure. Some corneal epithelial cells were enlarged with condensed nuclei surrounded by cytoplasmic vacuoles. The stroma showed some irregularly arranged widely spaced collagen fibers. In addition, disrupted Descemet's membrane and endothelium was observed in some fields (Figure 2c).

Sections from ADSCs treated subgroup (Subgroup II-c) revealed continuous regenerated surface epithelium with some enlarged vacuolated cells and intact thin Bowman's membrane. The substantia propria exhibited regular collagen bundles apart from some separated bundles with apparently normal keratocytes in between. Apparently normal Descemet's membrane with a layer of flattened continuous endothelial cells were also noticed (Figure 2d).

Sections from MSCs-EX treated subgroup (Subgroup II-d) showed almost complete restoration of the surface epithelium with thin intact Bowman's membrane. The substantia propria included neatly ordered collagen fibers, limited gaps, and normal keratocytes. Descemet membrane and endothelial cells appeared to be normal (Figure 2e).

Masson's Trichrome-Stained Sections

Group I revealed regular collagen bundles in the corneal stroma with continuous Bowman's & Descemet's membranes (Figure 3a). While sections from subgroup II-a showed separated epithelial tissue with disrupted Bowman's and Descemet's membranes, in addition to irregular separation of collagen bundles with loss of collagen from some parts of substantia propria (Figure 3b). Sections from subgroup II-b exhibited separated collagen fibers with newly formed blood vessels in between (Figure 3c). On the other hand, sections of subgroup II-c revealed stroma with more or less regular collagen bundles with minimal separation and continuous Bowman's & Descemet's membranes (Figure 3d). Finally, sections of subgroup II-d showed apparently normal stroma with regularly arranged collagen bundles, continuous Bowman's & Descemet's membranes (Figure 3e).

PAS-Stained Sections

Group I revealed an intense positive reaction in Bowman's membrane with magenta red color (Figures 4a,b), while both subgroups II-a & II-b displayed a weakly positive reaction in Bowman's membrane (Figures 4c,d respectively). Subgroup II-c showed a moderately positive reaction in Bowman's membrane (Figure 4e).

Finally, subgroup II-d depicted again strong reaction in Bowman's membrane (Figure 4f).

Immunohistochemical Results

Immunostaining for VEGF

There was mild positive cytoplasmic immunoreactivity within endothelial cells of the corneal sections of Group I (Figure 5a), Strong positive cytoplasmic immunoreaction within the endothelial lining of the blood vessels, keratocytes & corneal endothelial cells were detected in corneal sections of both subgroups II-a & II-b (Figures 5b,c respectively). However, cytoplasmic immunoreactivity of the vascular endothelial cells in the newly formed blood vessels was reduced in corneal sections of subgroup II-c (Figure 5d). There was mild positive immunoreactivity within endothelial cells of the corneal sections of subgroup II-d (Figure 5e).

Immunostaining for P53

Few positive immunoreactive nuclei within the epithelial cells were seen in corneal sections of group I (Figure 6a), while multiple positive immunoreactive nuclei within epithelial cells and keratocytes were seen in sections from both subgroups II-a & II-b (Figures 6b,c respectively). Reduced immunoreactivity was detected in the nuclei of epithelial cells & keratocytes in corneal sections of subgroup II-c (Figure 6d). Finally, few positive immunoreactive nuclei were detected within epithelial cells in corneal sections of subgroup II-d (Figure 6e).

Morphometric results (Table 1 and Histograms 1-5)

In H&E stained sections, the mean corneal thickness

values (in micrometers) showed a statistically significant increase in subgroup II-a compared to control and all treated subgroups. A significant increase was recorded in subgroup II-b compared to both subgroup II-c & subgroup II-d, in addition, a significant increase was detected in subgroup II-c compared to subgroup II-d. However, No statistically significant difference was detected between subgroup II-d and the control group.

The mean area % of collagen values revealed a significant increase in both subgroups II-a & II-b compared to group I, subgroup II-c & subgroup II-d. In addition, subgroup II-c showed a significant increase compared to group I & subgroup II-d. No statistically significant difference was detected between subgroups II-a & II-b and also between subgroup II-d and group I.

The mean gray of PAS reaction values indicated a significant decrease in both subgroups II-a & II-b compared to group I, subgroup II-c & subgroup II-d, in addition to a significant decrease in subgroup II-d compared to group I.

The mean number of VEGF immuno-positive cells indicated a significant increase in both subgroups II-a & II-b compared to control and other subgroups. Also, a non-significant increase was detected in both subgroups II-c & II-d when compared to group I

The mean number of P53 immuno-positive cells showed a significant increase in both subgroups II-a & II-b compared to control and other subgroups, in addition to a significant increase in subgroup II-c compared to group I.

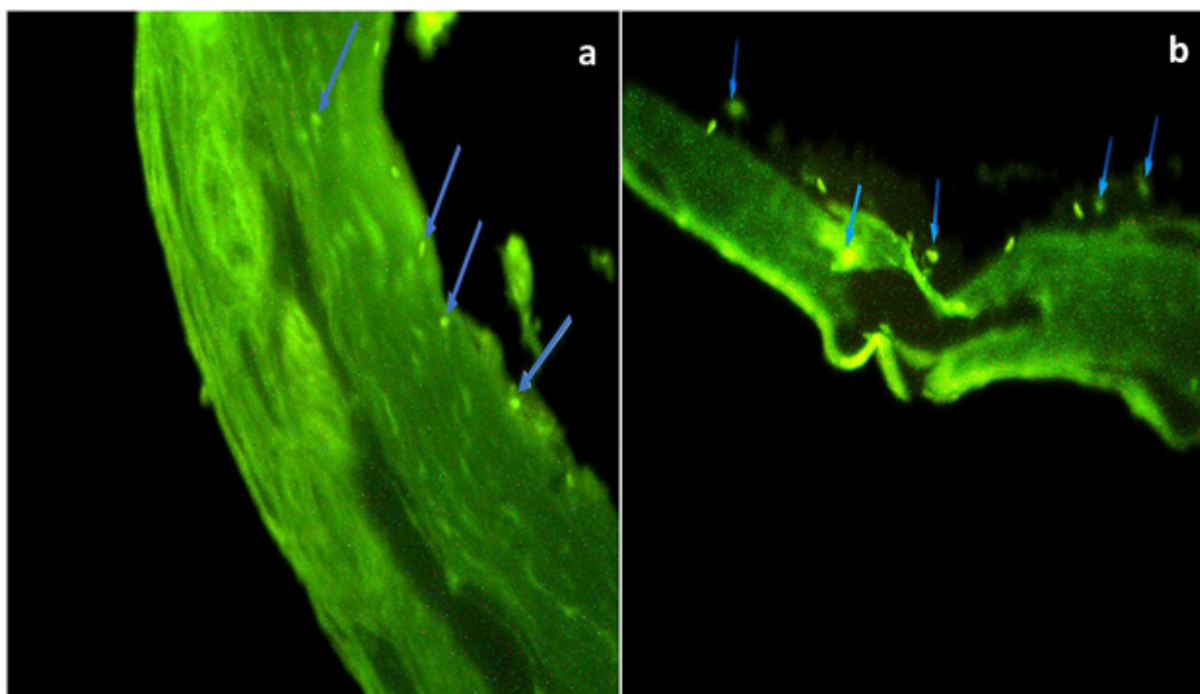


Fig. 1: Photomicrographs of corneal sections labeled with GFP immunofluorescence X200. (a) Subgroup II-c displays green positive immunofluorescent stem cells housed in the cornea (blue arrows). (b) Subgroup II-d reveals green positive immunofluorescent MSCs-EX housed in the cornea (blue arrows).

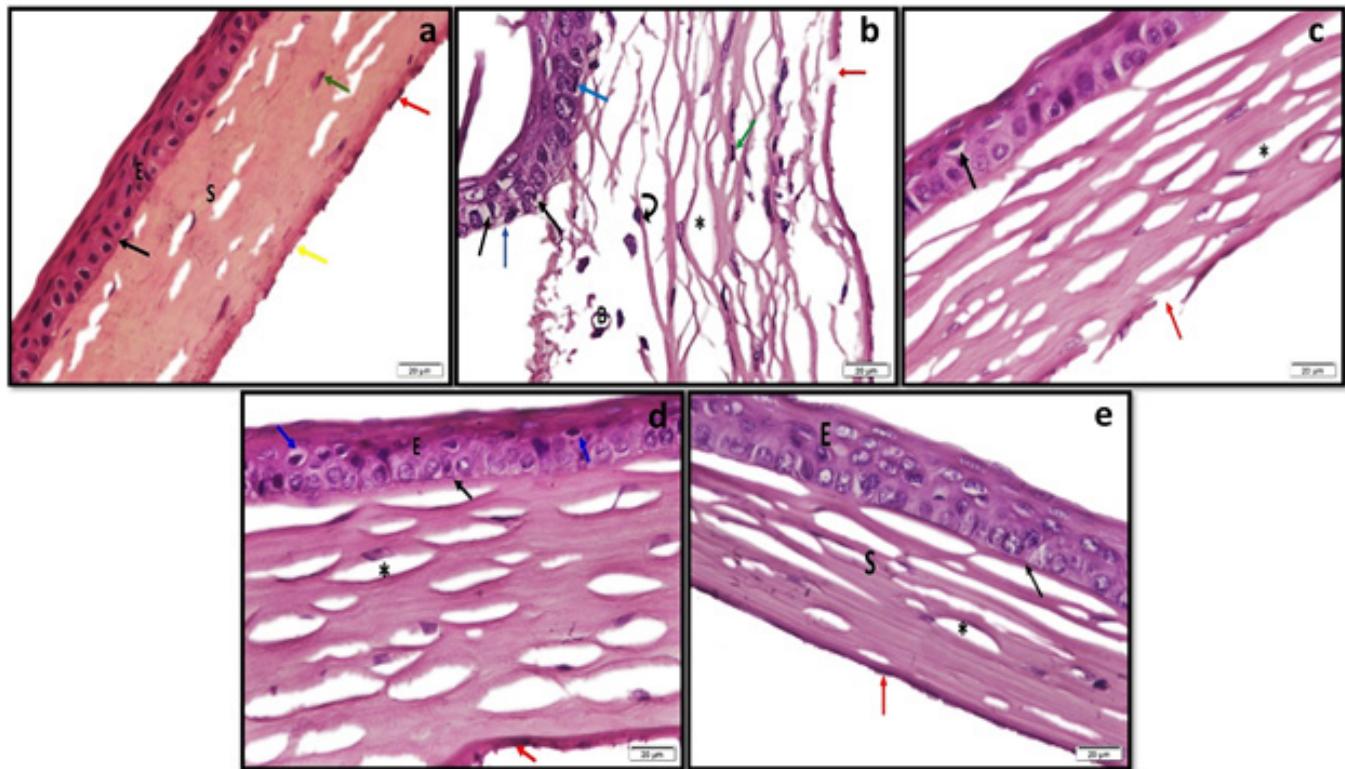


Fig. 2: Photomicrographs of sections from the central part of the cornea stained with H&E X 400. (a) Group I demonstrates normal structure of the cornea in the form of; corneal epithelium (E), a homogenous non cellular Bowman's membrane (black arrow), substantia propria (S) with regularly arranged collagen bundles and pale flattened nuclei of keratocytes scattered in-between (green arrows), a homogenous non cellular Descemet's membrane (yellow arrow) and a single layer of flattened endothelial cells with flattened nuclei (red arrow). (b) Subgroup II-a exhibits marked separation of corneal epithelium with flat basal cells (blue arrows). Some enlarged corneal epithelial cells with condensed nuclei that are surrounded by cytoplasmic vacuoles (black arrows) are observed. prominent widening & separation of the substantia propria (astrix) with multiple keratocytes exhibiting dark condensed nuclei (green arrow), neovascularization (B) and inflammatory cellular invasion (curved arrow) are also seen. The Descemet's membrane is disrupted and endothelial cells are lost in some parts (red arrow). (c) Subgroup II-b shows separation of the collagen bundles (astrix). Some enlarged corneal epithelial cells with condensed nuclei that are surrounded by cytoplasmic vacuoles (black arrow). Descemet's membrane & endothelial disruption is also noticed (red arrow). (d) Subgroup II-c shows continuous surface epithelium (E) with straight Bowman's membrane (black arrow). Collagen fibers of the stroma appeared regular although some are separated (astrix). Some enlarged corneal epithelial cells with dark condensed nuclei surrounded by cytoplasmic vacuoles (blue arrow). Descemet's membrane & its endothelium are almost normal (red arrow). (e) Subgroup II-d shows nearly complete restoration of surface epithelium (E) with thin intact Bowman's membrane (black arrow). Collagen fibers are regularly arranged (S) with some spaces in between (astrix). intact Descemet's membrane & endothelium are observed (red arrow).

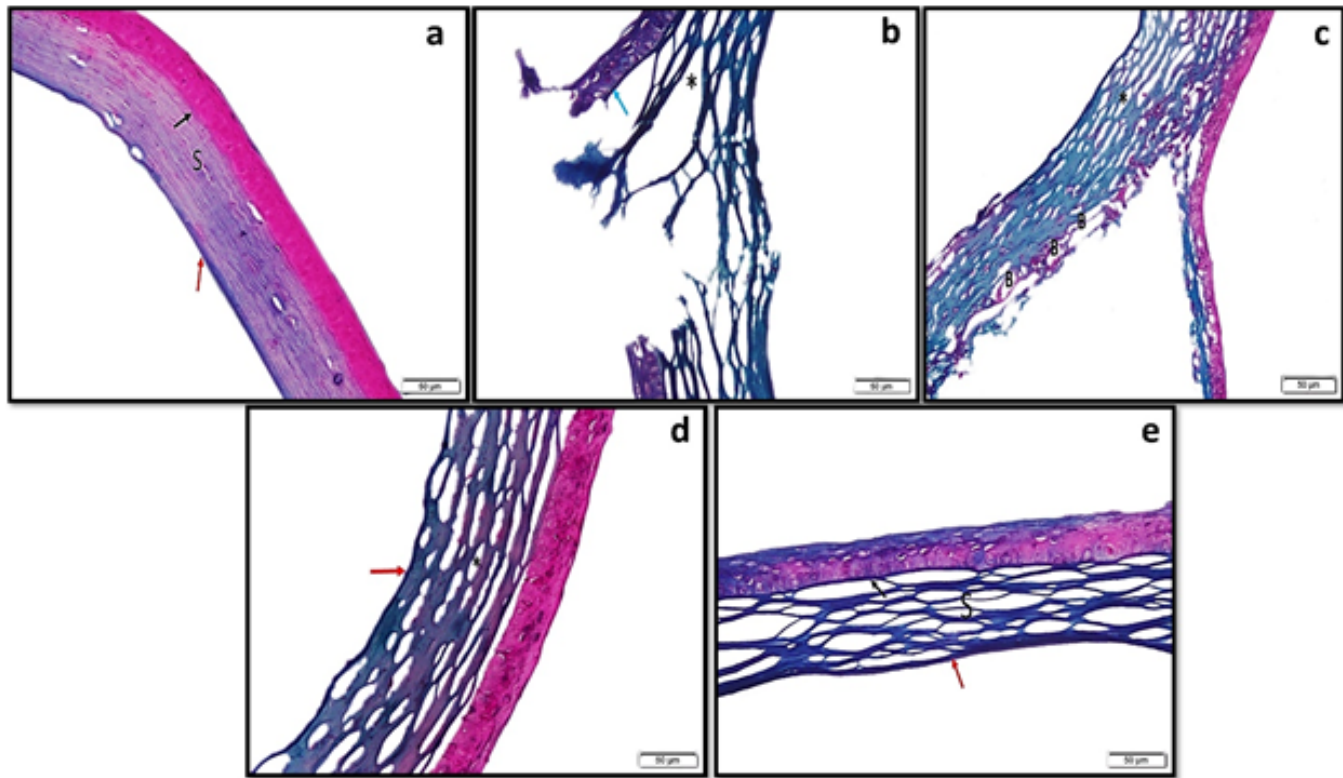


Fig. 3: Photomicrographs of sections from the central part of the cornea stained with Masson's trichrome X 200. (a) Group I shows continuous regular Bowman's membrane (black arrow) & Descemet's membrane (red arrow). Regularly arranged collagen fibers appear in the substantia propria (S). (b) Subgroup II-a exhibits complete epithelial tissue separation (blue arrow) from collagen fibers. Irregularly separated collagen bundles (asterisk) with loss of both Descemet's membrane and its endothelium are noticed. (c) Subgroup II-b demonstrates separated collagen fibers (asterisk) with newly formed blood vessels (B). (d) Subgroup II-c displays stroma with more or less regular collagen bundles although minimal separation of collagen fibers is still present (asterisk). A continuous Descemet's membrane (red arrow) is shown. (e) Subgroup II-d reveals substantia propria with regular collagen bundles (S), Regular Bowman's (black arrow) & Descemet's membranes (red arrow) are also seen.

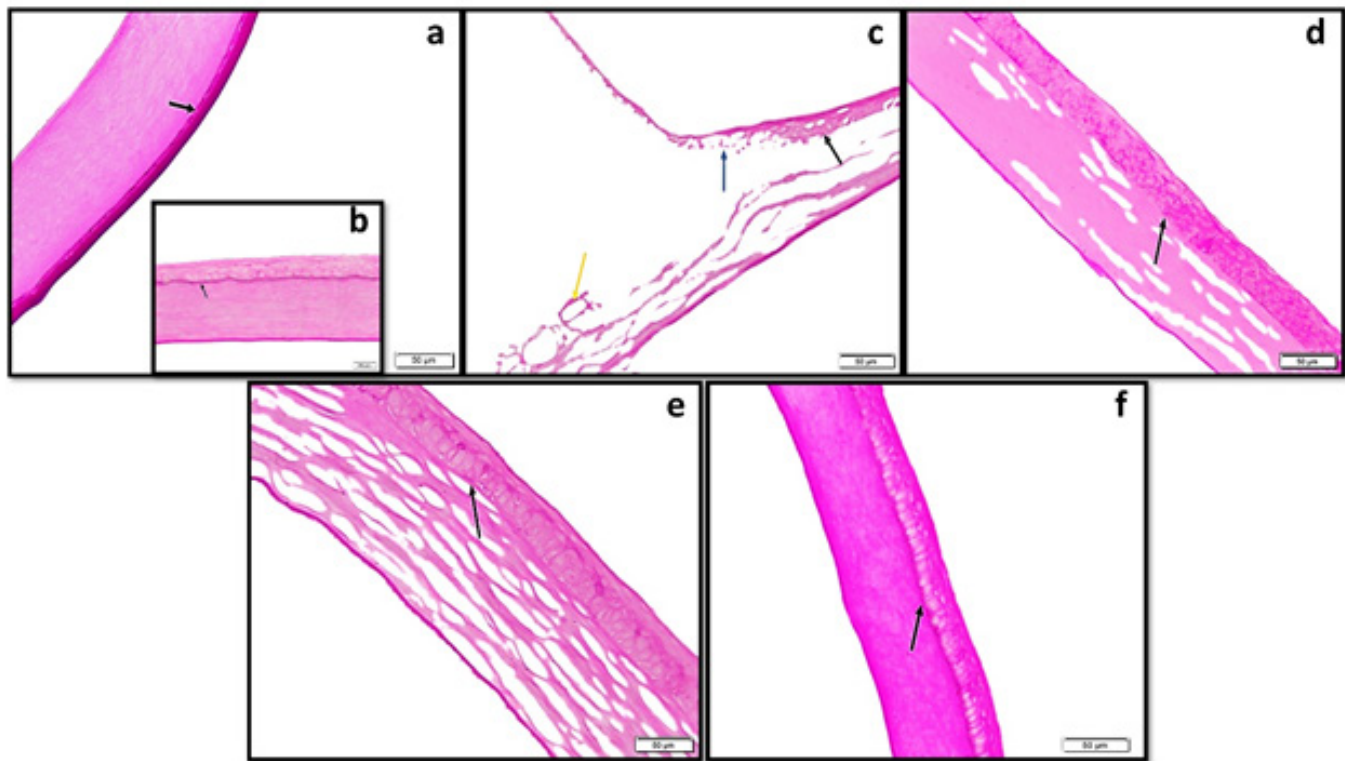


Fig. 4: Photomicrographs of sections from the central part of the cornea stained with PAS (a,c,d,e&f X200; b X400). (a) Group I shows intense positive PAS reaction in Bowman's membrane (black arrow) with a characteristic magenta red coloration. (b) Higher magnification of Group I. (c) Subgroup II-a shows weakly positive reaction in Bowman's membrane (black arrow) with marked separation of corneal epithelium (blue arrow) & positive reaction in the basement membrane of the newly formed blood vessels (yellow arrow). (d) Subgroup II-b shows weakly positive reaction in Bowman's membrane (black arrow). (e) Subgroup II-c shows moderately positive reaction in Bowman's membrane (black arrow). (f) Subgroup II-d shows intense positive reaction in Bowman's membrane (black arrow).

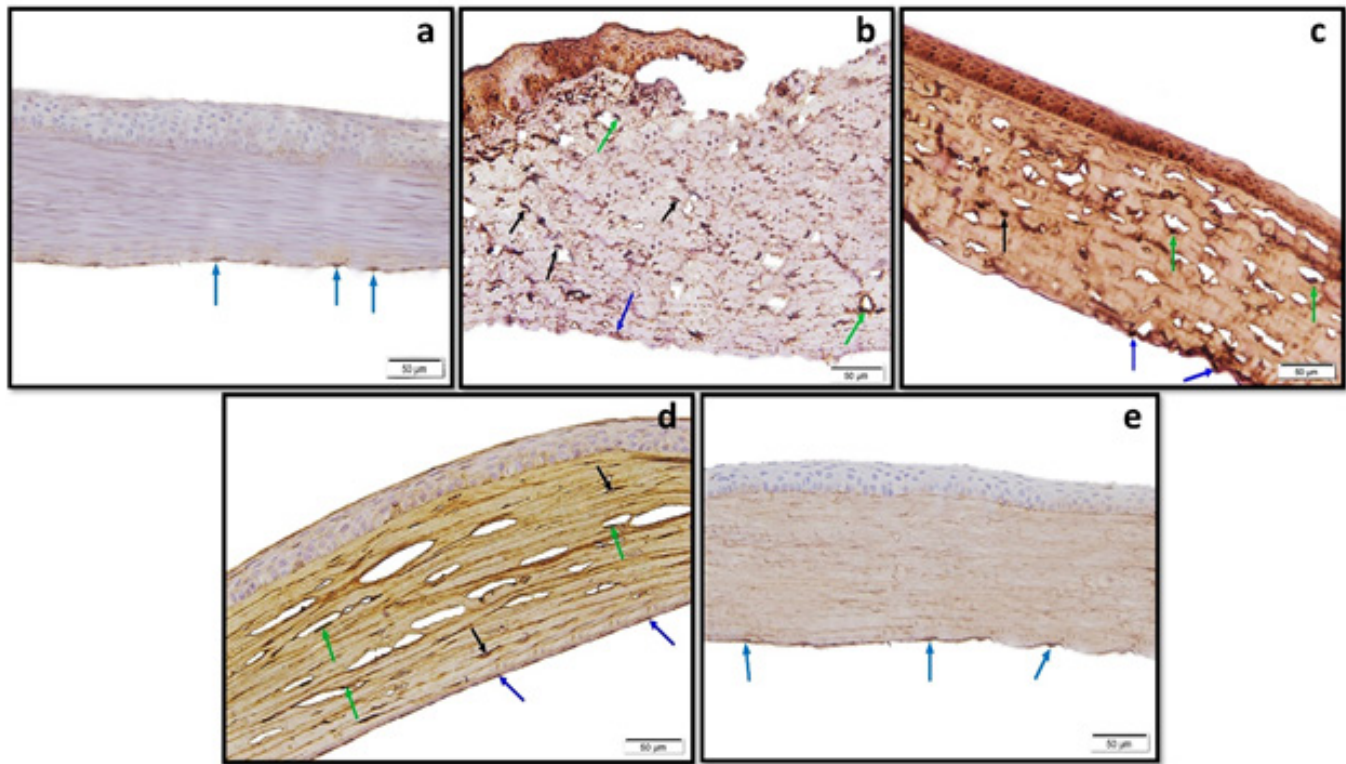


Fig. 5: Photomicrographs of sections from the central part of the cornea stained with VEGF immunostaining X200. (a) Group I shows mild cytoplasmic immunoreactivity within corneal endothelial cells (blue arrows). (b) & (c) Both subgroups II-a & II-b show strong positive immunoreactivity within the endothelial lining of the blood vessels (green arrows), keratocytes (black arrows) & corneal endothelial cells (blue arrows). (d) Subgroup II-c shows mild to moderate positive immunoreactivity within endothelial lining of blood vessels (green arrows), keratocytes (black arrows) & corneal endothelial cells (blue arrows). (e) Subgroup II-d shows mild immunoreactivity within the corneal endothelial cells (blue arrows).

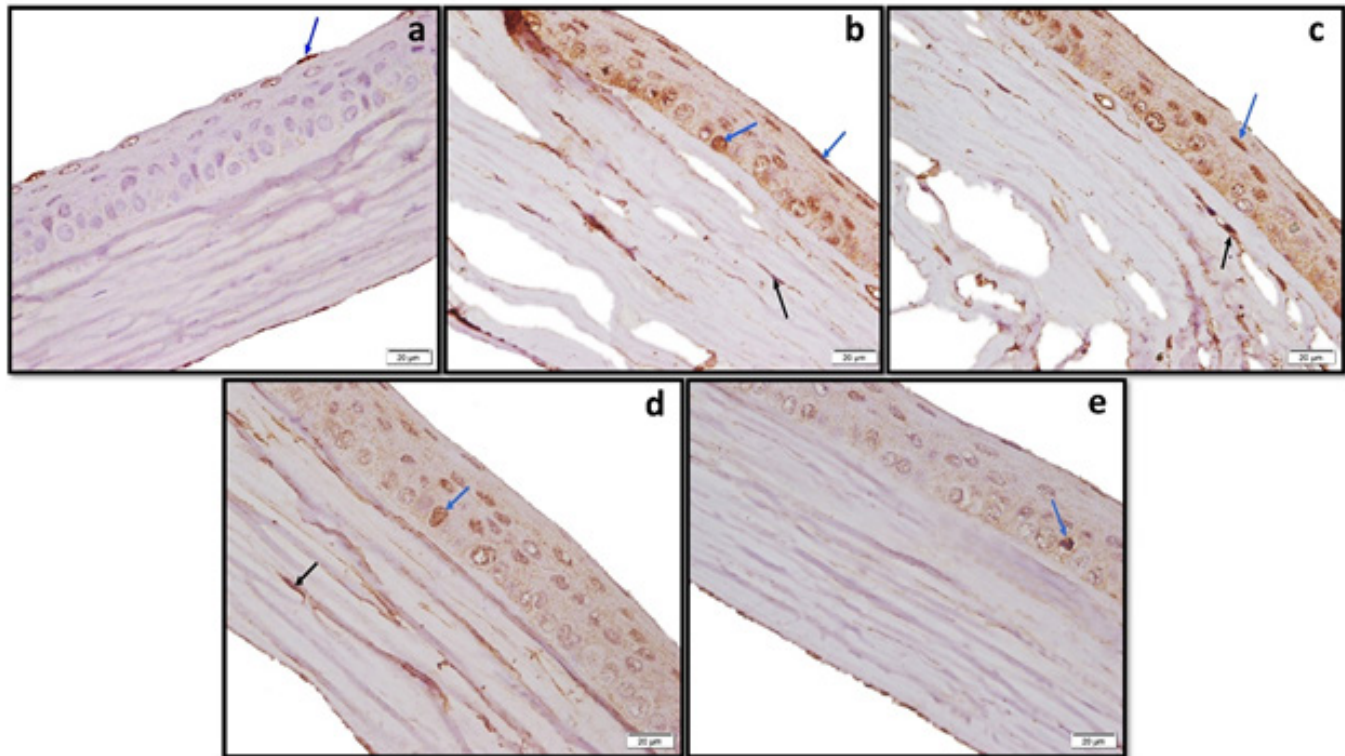


Fig. 6: Photomicrographs of sections from the central part of the cornea stained with P53 immunostaining X400. (a) Group I exhibits few positive nuclei within the superficial layer of corneal epithelial cells (blue arrow). (b) & (c) Subgroups II-a & II-b display multiple positive nuclei within the epithelial cells (blue arrows) and keratocytes (black arrows). (d) Subgroup II-c demonstrates reduced number of positive nuclei within epithelial cells (blue arrow) and keratocytes (black arrow). (e) Subgroup II-d shows few positive nuclei within corneal epithelial cells (blue arrow).

Table 1: Mean values \pm SD of morphometric parameters in the corneal sections of the studied groups

Group/Subgroup	Mean corneal thickness (μm)	Mean area% of collagen	Mean gray of PAS +ve reaction	Mean number of VEGF +ve cells	Mean number of P53 +ve cells
Group I	119.04 \pm 3.97	186.62 \pm 3.80	20.88 \pm 2.61	1.20 \pm 0.42	3.60 \pm 1.84
Subgroup II-a	214.07 \pm 3.23 ^{*S0^}	283.93 \pm 4.09 ^{*0^}	12.03 \pm 3.05 ^{*0^}	14.00 \pm 2.58 ^{*0^}	15.00 \pm 2.58 ^{*0^}
Subgroup II-b	153.49 \pm 3.63 ^{*#0^}	228.51 \pm 4.91 ^{*0^}	12.88 \pm 2.61 ^{*0^}	12.00 \pm 2.58 ^{*0^}	13.00 \pm 2.58 ^{*0^}
Subgroup II-c	126.39 \pm 3.24 ^{*#S^}	197.37 \pm 2.98 ^{*#S^}	16.68 \pm 2.29 ^{*#S0}	2.30 \pm 1.49 ^{#S}	6.60 \pm 1.84 ^{*#S^}
Subgroup II-d	121.52 \pm 2.70 ^{#S0}	183.59 \pm 3.80 ^{#S0}	18.66 \pm 2.24 ^{#S}	1.80 \pm 0.42 ^{#S}	2.60 \pm 1.84 ^{#S0}

Significance at $P < 0.05$

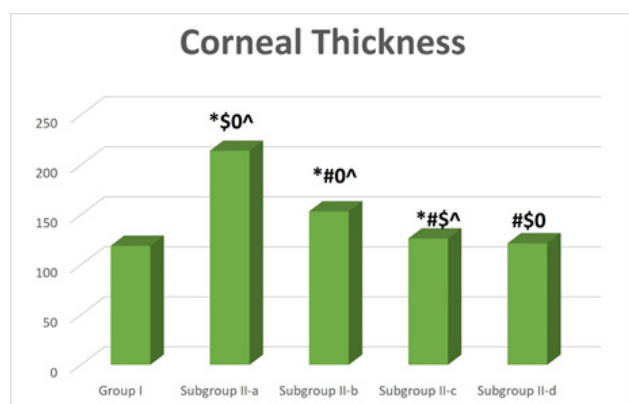
(*) Significant with control.

(#) Significant with Subgroup II-a.

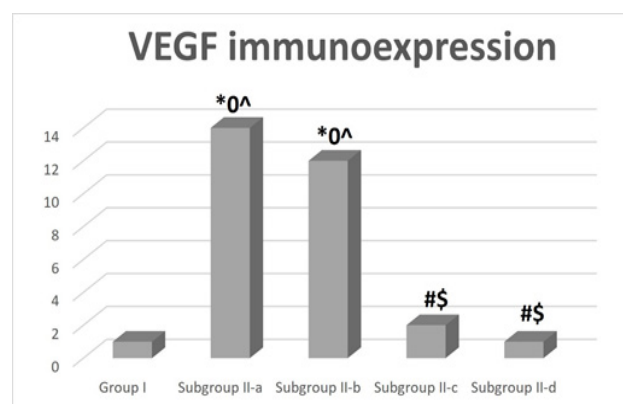
(S) Significant with Subgroup II-b.

(0) Significant with Subgroup II-c.

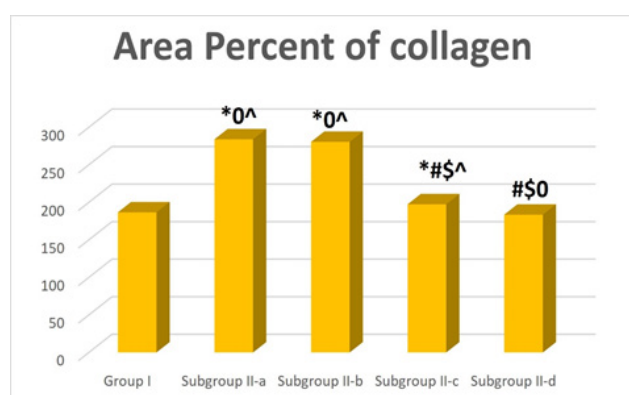
(^) Significant with Subgroup II-d.



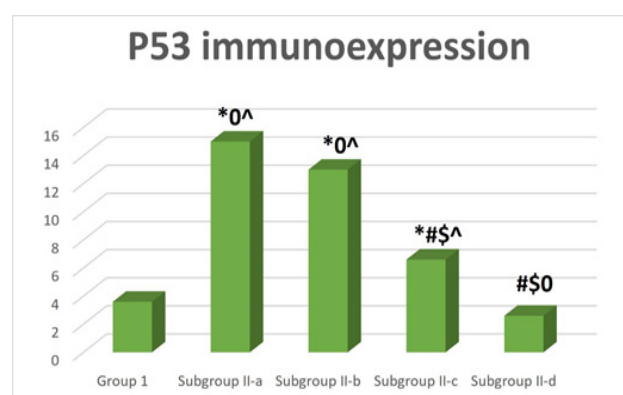
Histogram 1: Mean corneal thickness in the corneal sections of the studied groups: (*) Significant with control. (#) Significant with Subgroup II-a. (\$) Significant with Subgroup II-b. (0) Significant with Subgroup II-c. (^) Significant with Subgroup II-d.



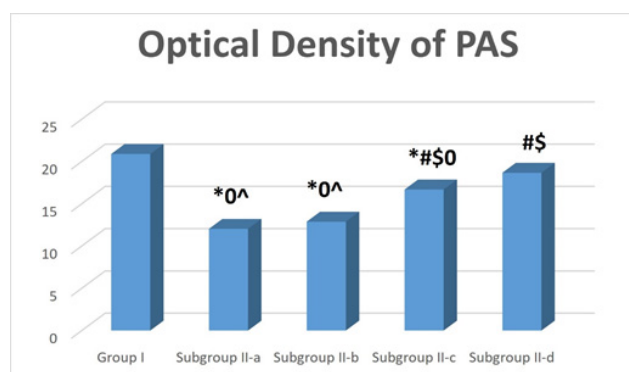
Histogram 4: Mean number of VEGF immuno-positive cells in the corneal sections of the studied groups: (*) Significant with control. (#) Significant with Subgroup II-a. (\$) Significant with Subgroup II-b. (0) Significant with Subgroup II-c. (^) Significant with Subgroup II-d.



Histogram 2: Mean area percent of collagen fiber content in the corneal sections of the studied groups: (*) Significant with control. (#) Significant with Subgroup II-a. (\$) Significant with Subgroup II-b. (0) Significant with Subgroup II-c. (^) Significant with Subgroup II-d.



Histogram 5: Mean number of P53 immuno-positive cells in the corneal sections of the studied groups: (*) Significant with control. (#) Significant with Subgroup II-a. (\$) Significant with Subgroup II-b. (0) Significant with Subgroup II-c. (^) Significant with Subgroup II-d.



Histogram 3: Mean gray of PAS reaction in the corneal sections of the studied groups: (*) Significant with control. (#) Significant with Subgroup II-a. (\$) Significant with Subgroup II-b. (0) Significant with Subgroup II-c. (^) Significant with Subgroup II-d.

DISCUSSION

Alkali burns are the most popular technique for studying corneal ulceration in lab animals^[30]. The goal of the current study was to assess and contrast the therapeutic effects of PRP, ADSCs, and MSCs-EX on rats with experimentally induced corneal alkali burn.

Corneal sections of subgroup II-a were examined to assess the progress of the healing process after induction of corneal alkali burn without receiving any treatment. They revealed marked epithelial changes ranging from desquamation to complete separation. Most basal & intermediate cells had karyolytic or pyknotic nuclei and vacuolated cytoplasm, which may indicate basal and supra-basal epithelial cells hydropic degeneration. This was in agreement with Chen *et al.*, (2017)^[31] who reported a dramatic rise in cell water content in epithelial cells surrounding the sloughed area which expanded the cell's

volume to cover a broad area during wound healing. In addition, basal cells lost their columnar appearance. The structural changes in the resting basement membrane may result in loss of their normal configuration. According to Abdelwahab *et al.*, (2017)^[32], basal cell and basement membrane hemi-desmosomal attachments disappear within a very short time over an area extending 50-70 μm from the corneal wound edge.

Inflammatory cellular infiltration, which affected normal corneal architecture, was also detected. El-Fattah El-Shazly & Ahmed (2016)^[33] clarified that neutrophils and macrophages invade the cornea after chemical damage. Inflammatory mediators released by macrophages induce corneal neovascularization (CNV), which is frequently associated with serious complications such as corneal edema, as confirmed by morphometric analysis which revealed a significant increase in corneal thickness when compared to the control group, in addition to inflammatory cellular infiltration, increased interstitial pressure with corneal scarring, eventually affect corneal transparency and cause blindness.

Corneal stroma also showed degenerated keratocytes between disrupted & widely spaced collagen fibers. Soliman *et al.*, (2015)^[34] mentioned that alkali burn stimulates the production of several angiogenic molecules as vascular endothelial growth factor (VEGF) and fibroblast growth factor, thereby enhancing corneal angiogenesis and stromal fibrosis which is supported by a statistically significant increase in collagen fibers area % and VEGF immun-expression when compared to the control group. Other investigators as Faruk *et al.*, (2017)^[35] & Lagali (2020)^[36] added that apoptosis and disappearance of the keratocytes concerned with collagen synthesis are the explanations for the disorganization and disruption of collagen fibers.

A significantly attenuated optical density of basement membrane of PAS-stained sections of the same subgroup was also noticed. This thinning could be due to collagen degradation as a consequence of the burn, in addition, Bowman's layer lacks keratocytes, causing its collagen turnover rates to be slow. It is possible that damage to the Bowman's layer caused all of the abnormal changes in the cornea and delayed the healing process of the epithelial defect. In agreement, Torricelli *et al.*, (2013)^[37] stated that Bowman's membrane acts as a barrier to inflammatory cytokine penetration from epithelium to the stroma (such as TGF-1) and possibly from the stroma to the epithelium (such as keratinocyte growth factor), so it is essential for homeostasis & wound healing of the cornea.

Hakami *et al.*, (2020)^[38] investigated how alkali burn caused apoptosis when applied to the cornea, which is in line with the current results which revealed a significant increase in P53 immunopositive cells in sections of subgroup II-a when compared to the control. According to their findings, alkali burn increased the alterations to the mitochondrial membrane and the release of cytochrome C, a mediator of apoptosis, leading to mitochondrial dysfunction.

Descemet's membrane was disrupted, resulting in loss of some endothelial cells. This finding coincided with Price *et al.*, (2021)^[39] who reported that either penetrating wounds or excessive corneal distortion (alkali burn) may harm the endothelium. Damage of the endothelial layer interferes with the mechanism that removes fluid from the stroma, which causes swelling and a loss of transparency in the wound area.

In the current work, rats of the PRP treated subgroup (Subgroup II-b) showed mild improvements as regard corneal histological structure, which was supported by morphometric analysis that showed a statistically significant decrease in corneal thickness when compared to subgroup II-a, with a statistically non-significant improvement in other parameters.

These findings contradict those of previous researchers such as Ibrahim and Elswaidy (2019)^[19] who suggested the effectiveness of early PRP intervention in alleviating corneal damage. That might be accounted for by the potent anti-inflammatory properties of PRP, which could quickly counteract the NaOH inflammatory effects. According to other researchers', PRP contains growth factors, such as transforming growth factor (TGF-1), epithelial growth factors, platelet-derived growth factors, fibroblast growth factors, insulin-like growth factor I, and vascular endothelial growth factors, as well as chemokines, cytokines, and newly produced active metabolites, were stored in the platelets' alpha-granules. These products are included in corneal stem cells migration, proliferation, and differentiation, which aids in the healing and maintenance of the ocular surface^[40].

It is reasonable that there must be strong factors suggested to be incriminated in this discrepancy between the results of the present work and the previous work's results, as for example, PRP preparation protocol and composition could have some effect. In terms of growth factor quantity and release kinetics, the technique used to prepare and activate PRP affects both its physical form and content^[41]. Also, concentration of platelets in the PRP prepare, repetitions of PRP doses all through the treatment period rather than single shot, duration of NaOH application to the cornea and the time between the ulcer induction and sacrifice. In addition, the design of the study may have a role in this discrepancy. Finally, previous works tested the effect of PRP alone in treating alkali burn, so they explain its effect as a good improvement, while the current study was intended to compare PRP's effect with that of ADSCs and MSCs-Ex, which had earned the last place in this comparison.

Treatment with ADSCs revealed moderate histological improvement of corneal ulcers in rats of subgroup II-c, confirmed by morphometric analysis in the form of a significant down-regulation of the corneal thickness, area percent of collagen fibers, both VEGF & P53 immun-expression with a significant increase in optical density of the PAS reaction when compared to subgroup II-a.

For many reasons, the potential therapeutic benefits of ADSCs have been valued in regenerative therapies. They are highly capable of developing along the mesodermal, ectodermal, and endodermal lineages into mature cells. They are less invasive, easier to harvest, and more productive to grow^[7]. Because it is a simple and straightforward procedure for ophthalmologists, ADSCs subconjunctival injection is one of the popular clinical treatment routes^[4]. Our study found that alkali burn corneas treated with ADSCs showed homing of GFP labelled MSCs to the injury site, this finding corroborates the previous reports as Almaliotis *et al.*, (2015)^[42] on MSCs permeation after sub-conjunctival administration.

This work's findings are consistent with those of Harkin *et al.* (2015)^[43], who stated that MSCs improved epithelial healing and repaired corneal damage through a variety of processes, including the secretion of cytokines and growth factors that regulated cell signaling and proliferation after corneal alkali burn. Another study confirmed that epithelial defects in damaged corneas treated with MSCs showed considerable improvement and closure, resulting in well-organized layers of epithelium with few intercellular gaps. MSCs enable remnant corneal epithelial cells to recapture the stem cell niche in the cornea or to develop into corneal stromal cells (keratocytes). Chemo-cytokines released as a result of stress, such as burn, cause stem cells to migrate and localize in specific tissues. Furthermore, these substances promote the mobilization of endogenous MSCs into peripheral blood^[35].

Furthermore, keratan-sulfate proteoglycans released by regenerated keratocytes aid in the preservation of the organized stromal structure. Keratocytes are necessary for corneal transparency because they produce and maintain normal collagen interfibrillar spacing and fibril width^[44].

El-Din *et al.*, (2021)^[45] hypothesized that MSCs therapy improved wound healing and corneal surface regeneration through its anti-inflammatory properties, in the form of suppression of CD45, IL-2, and MMP2 expression. On the other hand, the adaptive CD4+ T cell invasion was blocked, as well as the expression of MMP2 and cytokines associated with CD4+ T cells, which may have been suppressed by the release of soluble agents.

Treatment with MSCs-EX showed improvement in all parameters. There were well organized and continuous stratified squamous epithelium, almost normal keratocytes between reconstructed corneal stromal arrangement with reduced neovascularization and no inflammatory cell's invasion. A continuous Descemet's membrane with endothelial cells, in addition to reduced number of apoptotic nuclei were also detected. These dramatic improvements were confirmed by morphometric analysis which showed almost no statistical differences in all parameters measured when compared to the control group.

Previous investigators as Han *et al.*, 2017^[46] demonstrated that histological and ultrastructural changes of corneal epithelial cells and keratocytes may be influenced

by exosomes, which would then allow the cells to change their activities. Many authors as Yao & Bai, (2013)^[47] & Vizoso *et al.*, (2017)^[48] accepted that they may have a significant impact on the regulation of many physiological processes by promoting the anti-inflammatory cytokines release, reducing angiogenesis through reduction of VEGF, immune activation, cell plasticity, and regenerative abilities.

To maintain corneal avascularity, the ratio of angiogenic to anti-angiogenic factors in the corneal epithelium must be tightly regulated. Exosomes carried proteins important for CNV and wound healing, such as thrombospondin-2, which is often expressed on avascular tissues like the cornea and is involved in numerous cellular processes^[49,46].

Some investigators as Shen *et al.*, (2016)^[50] recommended that exosomes are used in large quantities in MSCs-EX based therapies, which may be important to their mechanisms of action and make them superior to stem cells in by inhibiting the release of endogenous cytokines and other pathogenic substances that are generated as a result of different types of induced injuries. Exosome administration is safer than stem cell administration, and MSCs-EXs nano-dimensional size can make it simple for them to pass through biological barriers and enter the target organs, giving them many advantages over stem cells. Exosomes can also be preserved without losing their ability to function. Therefore, exosomes are more advantageous than stem cells for use in treating diseases^[51,11,12].

CONCLUSION

In conclusion, this study provides experimental evidence ensuring the better therapeutic effect of treatment with (MSCs-EXs) than (ADSCs & PRP) in a rat model of experimentally induced corneal alkali burn.

ACKNOWLEDGMENTS

Professor Laila Ahmed Rashed, Department of Biochemistry, Faculty of Medicine, Cairo University, Egypt performed PRP, ADSCs & MSCs-EX preparation. Ms. Mervat Morqous technician at Medical Histology and Cell Biology Department contributed to specimens' preparation.

CONFLICT OF INTERESTS

There are no conflicts of interest.

REFERENCES

1. Sharma N, Kaur M, Agarwal T, Sangwan VS, Vajpayee RB: Treatment of acute ocular chemical burns in Survey of ophthalmology (2018);63(2): 214-235. DOI: 10.1016/j.survophthal.2017.09.005.
2. Kandeel S, Balaha M: Olopatadine enhances recovery of alkali-induced corneal injury in rats in Life sciences (2018);207: 499-507. DOI: 10.1016/j.lfs.2018.07.002.
3. Li M, Chen Z, Liu L, Ma X, Zou J: Topical Vitamin C Promotes the Recovery of Corneal Alkali Burns in Mice in Journal of Ophthalmology (2021);2021: 1-10. DOI: 10.1155/2021/2406646

4. El-Mahalaway AM, El-Azab NEE, Abdrabbo M, Said OM, Sabry D, El Sibaie MM: Comparative light and electron microscopic study on the therapeutic efficacy of adipose derived stem cells versus exosomes for experimentally induced acute corneal injuries in rats in *Stem Cell Res Ther.* (2018);8(431): 1-12. DOI: 10.4172/2157-7633.100043.
5. Girgin M, Binnetoglu K, Duman K, Kanat BH, Cetinkaya Z, Ayten R, Ilhan YS, Ilhan N, Seker I, Timurkaan N: Effects of platelet rich plasma on fascial healing in rats with fecal peritonitis in *Acta chirurgica brasileira* (2016);31: 314-319. DOI: 10.1590/S0102-865020160050000004.
6. Circi E, Akman YE, Sukur E, Bozkurt ER, Tuzuner T, Ozturkmen Y: Impact of platelet-rich plasma injection timing on healing of Achilles tendon injury in a rat model in *Acta Orthop Traumatol Turc.* (2016);50(3): 366-372. DOI: 10.3944/AOTT.2015.15.0271.
7. Frese L, Dijkman PE, Hoerstrup SP: Adipose tissue-derived stem cells in regenerative medicine in *Transfusion Medicine and Hemotherapy* (2016);43(4): 268-274. DOI: 10.1159/000448180.
8. Omar AI: Influence of rat adipose tissue-derived mesenchymal stem cells on brain tissues following permanent unilateral common carotid artery occlusion in adult male albino rat: a histological and immunohistochemical study in *The Egyptian Journal of Histology* (2016);39(3): 241-259. DOI: 10.1097/01.EHX.0000490000.86687.5c.
9. Omar FR, Amin NMA, Elsherif HA, Mohamed D: Role of adipose derived stem cells in restoring ovarian structure of adult albino rats with chemotherapy-induced ovarian failure: a histological and immunohistochemical study in *J Carcinog Mutagen* (2016);7(254): 1-12. DOI:10.4172/2157-2518.1000254.
10. Mead B, Tomarev S: Bone marrow-derived mesenchymal stem cells-derived exosomes promote survival of retinal ganglion cells through miRNA-dependent mechanisms in *Stem cells translational medicine* (2017);6(4): 1273-1285. DOI: 10.1002/scnm.16-0428.
11. Yu B, Shao H, Su C, Jiang Y, Chen X, Bai L, Zhang Y, Li Q, Zhang X, Li X: Exosomes derived from MSCs ameliorate retinal laser injury partially by inhibition of MCP-1 in *Scientific reports* (2016);6(1): 1-12. DOI:10.1038/srep34562.
12. Omar SS: Mesenchymal Stem Cells for Treating Ocular Surface Diseases in *J Stem Cell Res.* (2017);1: 1-6. DOI: 10.1186/s12886-015-0138-4.
13. Salem M, Helal O, Metwaly H, El Hady A, Ahmed S: Histological and immunohistochemical study of the role of stem cells, conditioned medium and microvesicles in treatment of experimentally induced acute kidney injury in rats in *Journal of Medical Histology* (2017);1(1): 69-83. DOI: 10.21608/jmh.2017.1108.1018.
14. Sayed AA, EL-Deek SE, EL-Baz MA, Sabry D, Al-Rageacy A, Mansey A, Meligy F, Abdelaziz K: Exosomes derived from bone marrow mesenchymal stem cells restore cisplatin induced ovarian damage by promoting stem cell survival, meiotic, and apoptotic markers in *Glo Adv Res J Med Med Sci.* (2017);6(6): 116-130. <http://garj.org/garjmmms>
15. Kim EC, Kim TK, Park SH, Kim MS: The wound healing effects of vitamin A eye drops after a corneal alkali burn in rats in *Acta ophthalmologica* (2012);90(7): e540-e546. DOI: 10.1111/j.1755-3768.2012.02496.x
16. Ibrahim M, Elswaidy N: A histological and immunohistochemical study of the effect of platelet-rich plasma on a corneal alkali burn in adult male albino rat in *Egyptian Journal of Histology* (2019);42(2): 482-495. DOI: 10.21608/ejh.2019.7018.1059
17. Safwat A, Sabry D, Ragiae A, Amer E, Mahmoud RH, Shamardan RM: Adipose mesenchymal stem cells-derived exosomes attenuate retina degeneration of streptozotocin-induced diabetes in rabbits in *Journal of circulating biomarkers* (2018);7: 1-10. DOI: 10.1177/1849454418807827
18. Nasser S, Morcos M, Gazia MA, Yousry M, Osman A: Comparative Histological Study on the Effect of Early and Late Administration of Adipose Derived Stem Cells on Corneal Alkali Burn in Adult Male Albino Rats in *Egyptian Journal of Histology* (2019); 42(3): 635-650. DOI: 10.21608/EJH.2019.7024.1060
19. Ebrahim N, Mohammed O, Dessouky AA, Abdel Fatah DS: The potential therapeutic effect of stem cells loaded on two different vehicles (amniotic membrane and platelet rich plasma gel) in experimentally induced corneal alkali burns in rats in *Egyptian Journal of Histology* (2017);40(4): 405-426. DOI: 10.21608/EJH.2017.5511
20. Sonleitner D, Huemer P, Sullivavan DY: A simplified technique for producing Platelet-Rich Plasma and Platelet Concentrate for intraoral bone grafting techniques: A technical note in *International J of Oral and Maxillofacial Implants* (2000);15:879-882. PMID: 11151589.
21. Danysz W, Han Y, Li F, Nicoll J, Buch P, Hengl T, Ruitenber M, Parsons C: Browning of white adipose tissue induced by the ss3 agonist CL-316,243 after local and systemic treatment-PK-PD relationship in *Biochimica Biophysica Acta (BBA)-Molecular Basis of Disease* (2018);1864(9), 2972-2982. DOI: 10.1016/j.bbadis.2018.06.007

22. Liu M, Yang Y, Zhao B, Yang Y, Wang J, Shen K, Yang X, Hu D, Zheng G, Han J: Exosomes Derived from Adipose-Derived Mesenchymal Stem Cells Ameliorate Radiation-Induced Brain Injury by Activating the SIRT1 Pathway in Front Cell Dev Biol. (2021);9: 693782. DOI: 10.3389/fcell.2021.693782
23. Hussein EN, Hame, GM, Seif AA, Ahmed MA, Abu Zahra FAE: Effects of Mesenchymal Stem Cells Therapy on Cardiovascular Risk Factors in Experimental Diabetic Kidney Disease in Canadian Journal of Kidney Health and Disease (2020);7: 20-39. DOI: 10.1177/2054358120957429
24. Pourghasem M, Naisiri E, Shafi H: Early renal histological changes in Alloxan – induced diabetic rats in International Journal of Molecular Cell Med. (2014);3: 11 – 15. PMID: 24551816; PMCID: PMC3927393
25. Kiernan JA: Histological and histochemical methods: Theory and Practice. 5th ed., Scion Publishing Ltd. (2015) pp: 144-146.
26. Bancroft J and Gamble M: Staining methods. Theory and Practice of Histological Techniques. 7th ed., Edinburgh, London, Madrid, Melbourne, New York, Tokyo: Churchill Livingstone. (2008) pp. 121–35. 263-325.
27. Suvarna SK, Layton C and Bancroft JD: Bancroft's Theory and Practice of Histological Techniques. 7th ed., New York, USA: Elsevier Health Sciences, Churchill Livingstone; (2012) pp. 215–239.
28. Kerr JB, Duckett R, Myers M: Quantification of healthy follicles in the neonatal and adult mouse ovary: evidence for maintenance of primordial follicle supply in Reproduction (2006);132(1): 95-109. DOI: 10.1530/rep.1.01128
29. Emsley R, Dunn G, White IR: Mediation and moderation of treatment effects in randomized controlled trials of complex interventions in Start Methods Med Res. (2010); 19(3): 237-270. DOI:10.1177/0962280209105014
30. Gao M, Sang W, Liu F: High MMP-9 expression may contribute to retroprosthetic membrane formation after kpro implantation in rabbit corneal alkali burn model in J Ophthalmology (2016); 1-8. DOI: 10.1155/2016/1094279
31. Chen J, Lan J, Liu D, Backman LJ, Zhang W, Zhou Q, Danielson P: Ascorbic acid promotes the stemness of corneal epithelial stem/progenitor cells and accelerates epithelial wound healing in the cornea in Stem Cells Translational Medicine (2017); 6(5): 1356-1365. DOI: 10.1002/sctm.16-0441
32. Abdelwahab S, El-Hameed A, Saber E, Sayed A: Role of vitamin A in the healing process of alkali caused corneal injury of adult male albino rat: Histological and immunohistochemical study in Journal of Medical Histology (2017); 1(1): 57-68. DOI: 10.21608/jmh.2017.1020.1014
33. El-Fattah El-Shazly AA, Ahmed AI: Therapeutic effects of extracts from spirulina platensis versus bevacizumab on inflammation-associated corneal neovascularization in J Med Surg Pathol (2016); 1(102): 1-7. DOI:10.4172/jmsp.1000102
34. Soliman ME, Mahmoud BL, Kafafy MA, ElHaroun HM, Mohamed DM: Histological changes in cornea following repeated exposure to benzalkonium chloride and the possible protective effect of topically applied sodium hyaluronate in Nat. Sci (2015);13(5): 64-76. <http://www.sciencepub.net/nature>.
35. Faruk EM, Mansy AE, Al-Shazly AM, Taha NM: Light and Electron Microscopic Study of the Anti-Inflammatory Role of Mesenchymal Stem Cell Therapy in Restoring Corneal Alkali Injury in Adult Albino Rats in J. stem cell Bio. Transplant (2017);1 (1): 1-8. DOI: 10.1155/2020/4127959
36. Lagali N: Corneal stromal regeneration: current status and future therapeutic potential in Current Eye Research (2020); 45(3): 278-290. DOI: 10.1080/02713683.2019.1663874
37. Torricelli AA, Singh V, Santhiago MR, Wilson SE: The corneal epithelial basement membrane: structure, function, and disease in Investigative ophthalmology & visual science (2013); 54(9): 6390-6400. DOI:10.1167/iovs.13-12547
38. Hakami NY, Disting GJ, Chan EC, Shah MH, Peshavariya HM: Wound healing after alkali burn injury of the cornea involves Nox4-type NADPH oxidase in Investigative ophthalmology & visual science (2020); 61(12): 20-27. DOI:10.1167/iovs.61.12.20
39. Price MO, Mehta JS, Jurkunas UV, Price Jr FW: Corneal endothelial dysfunction: Evolving understanding and treatment options in Progress in Retinal and Eye Research (2021); 82: 100904. DOI: 10.1016/j.preteyeres.2020.100904
40. Alio JL, Rodriguez AE, Abdelghany, Oliveira RF: Autologous platelet-rich plasma eye drops for the treatment of post-LASIK chronic ocular surface syndrome in Journal of ophthalmology (2017); 2457620. DOI: 10.1155/2017/2457620
41. Cavallo C, Roffi A, Grigolo B, Mariani E, Pratelli L, Merli G, Kon E, Marcacci M, Filardo G: Platelet-rich plasma: the choice of activation method affects the release of bioactive molecules in BioMed Research International (2016); 2016: 1-7. DOI: 10.1155/2016/6591717
42. Almaliotis D, Koliakos G, Papakonstantinou E, Komnenou A, Thomas A, Petrakis S, Nakos I, Gounari E, Karampatakis V: Mesenchymal stem cells improve healing of the cornea after alkali injury in Graefes Archive for Clinical and Experimental Ophthalmology (2015); 253(7): 1121-1135. DOI: 10.1007/s00417-015-3042-y

43. Harkin DG, Foyl L, Bray LJ, Sutherland AJ, Li FJ, Cronin BG: Concise reviews: can mesenchymal stromal cells differentiate into corneal cells? A systematic review of published data in *Stem Cells* (2015); 33(3): 785-791. DOI: 10.1002/stem.1895
44. Holan V, Trosan P, Cejka C, Javorkova E, Zajicova A, Hermankova B, Chudickova M, Cejkova J: A comparative study of the therapeutic potential of mesenchymal stem cells and limbal epithelial stem cells for ocular surface reconstruction in *Stem cells translational medicine* (2015); 4(9): 1052-1063. DOI:10.5966/sctm.2015-0039
45. El-Din WN, Nooreldin N, Essawy AS: The potential therapeutic efficacy of intravenous versus subconjunctival mesenchymal stem cells on experimentally ultraviolet-induced corneal injury in adult male albino rats in *Folia Morphologica* (2021): 1-45. DOI: 10.5603/FM.a2021.0085
46. Han KY, Tran JA, Chang JH: Potential role of corneal epithelial cell derived exosomes in corneal wound healing and neovascularization in *Sci Rep* (2017); 7:1-14. DOI: 10.1038/srep40548
47. Yao L, Bai H: Mesenchymal stem cells and corneal reconstruction in *Molecular vision* (2013); 19: 2237-2243. <http://www.molvis.org/molvis/v19/2237>
48. Vizoso FJ, Eiro N, Cid S, Schneider J, Perez-Fernandez R: Mesenchymal stem cell secretome: toward cell-free therapeutic strategies in regenerative medicine in *International journal of molecular sciences* (2017); 18(9): 1852. DOI: 10.3390/ijms18091852
49. Huang L, Ma W, Ma Y, Feng D, Chen H, Cai B: Exosomes in mesenchymal stem cells, a new therapeutic strategy for cardiovascular diseases? In *International Journal of Biological Sciences* (2015); 11(2): 238. DOI: 10.7150/ijbs.10725.
50. Shen B, Liu J, Zhang F, Wang Y, Qin Y, Zhou Z, Qiu J, Fan Y: CCR2 positive exosome released by mesenchymal stem cells suppresses macrophage functions and alleviates ischemia/reperfusion-induced renal injury in *Stem cells international* (2016); 2016: 1-9. DOI: 10.1155/2016/1240301
51. Rani S, Ryan AE, Griffin MD, Ritter T: Mesenchymal stem cell-derived extracellular vesicles: toward cell-free therapeutic applications in *Molecular Therapy* (2015); 23(5): 812-823. DOI:10.1038/mt.2015.44

المخلص العربي

دراسة هستولوجية وهستوكيميائية مناعية مقارنة على تأثير البلازما الغنية بالصفائح الدموية والخلايا الجذعية المستخلصة من النسيج الدهني والحوصلات المستخلصة من الخلايا الجذعية الوسطية على حروق القرنية القلوية المحدثة في الجرذان البيضاء

سحر عزت نصر، أمل الهام فارس، ايمان احمد السيد، أسماء احمد الشافعي

قسم الأنسجة الطبية وبيولوجيا الخلية، كلية الطب، جامعة القاهرة، مصر

الخلفية والأهداف: يمكن أن يكون الضرر القلوي للقرنية كارثيًا وينتج عنه ألم مدى الحياة وفقدان بصري. وقد كان الهدف من هذا العمل هو البحث والمقارنة بين التأثيرات العلاجية المحتملة للبلازما الغنية بالصفائح الدموية، والخلايا الجذعية المشتقة من الأنسجة الدهنية، والحوصلات المستخلصة من الخلايا الجذعية الوسيطة على حروق القرنية القلوية المستحدثة تجريبيا في الجرذان.

المواد والطرق: تم تقسيم ٦٠ جرذًا من الذكور البالغين إلى: مجموعة متبرعة. ١٠ جرذان، المجموعة الأولى (المجموعة الضابطة)؛ ١٠ جرذان، والمجموعة الثانية (مجموعة حرق القرنية القلوي)؛ ٤٠ جرذ. تلقت جميع جرذان المجموعة الثانية بالعين اليمنى حرق قلوي بالقرنية بواسطة هيدروكسيد الصوديوم، ثم تم تقسيمها بالتساوي إلى: المجموعة الفرعية ٢-أ (مجموعة فرعية للتعافي التلقائي): تركت دون علاج، المجموعة الفرعية ٢-ب (مجموعة فرعية معالجة بالبلازما الغنية بالصفائح الدموية): تلقت حقنة واحدة تحت الملتحمة من ٠,٥ مل من البلازما الغنية بالصفائح الدموية بعد ساعتين من الحرق القلوي للقرنية، المجموعة الفرعية ٢-ج (المجموعة الفرعية المعالجة بالخلايا الجذعية المشتقة من الأنسجة الدهنية): تلقت حقنة واحدة تحت الملتحمة من ١,٣ × ١٠٥ من الخلايا الجذعية المشتقة من الأنسجة الدهنية؛ بعد ساعة واحدة من الحرق القلوي للقرنية والمجموعة الفرعية ٢-د (المجموعة الفرعية المعالجة بالحوصلات المستخلصة من الخلايا الجذعية الوسيطة): تلقت حقنة واحدة تحت الملتحمة من ١٠٠ ميكروغرام بروتين / مل من الحوصلات المستخلصة من الخلايا الجذعية الوسيطة؛ ١ ساعة بعد الحرق القلوي للقرنية. تم التضحية بالجرذان بعد ٣ أسابيع، ثم تم استئصال قرنية العين اليمنى للتحليل النسيجي والمورفومتري والإحصائي.

النتائج: تم الكشف عن تدهور البنية النسيجية للقرنية في المجموعة الفرعية ٢-أ، في شكل تلف وتقرن الخلايا الظهارية والبطانية للقرنية، تدهور الخلايا القرنية وتهتك سدق القرنية مع تشكل الأوعية الدموية الجديدة والتسلل الخلوي. أظهر العلاج باستخدام البلازما الغنية بالصفائح الدموية، والخلايا الجذعية المشتقة من الأنسجة الدهنية، والحوصلات المستخلصة من الخلايا الجذعية الوسيطة درجات مختلفة من التحسن، في شكل تجديد ظهارة القرنية والبطانة وسدى القرنية مع اختفاء الأوعية الدموية الجديدة والتسلل الخلوي.

الاستنتاج: أظهر العلاج باستخدام البلازما الغنية بالصفائح الدموية، والخلايا الجذعية المشتقة من الأنسجة الدهنية، والحوصلات المستخلصة من الخلايا الجذعية الوسيطة تحسناً بشكل كبير في التغيرات التنكسية القرنية التي يسببها الحرق القلوي من خلال خصائصها المضادة للالتهابات والمضادة لتولد الأوعية ومضادات موت الخلايا المبرمج؛ مع تحسن أكثر وضوحاً للعلاج بالحوصلات المستخلصة من الخلايا الجذعية الوسيطة.